Graduate School of Oceanography Faculty Publications

Graduate School of Oceanography

3-2-2020

Variability approaching the thermal limits can drive diatom community dynamics

Stephanie Anderson

Tatiana A. Rynearson
University of Rhode Island, rynearson@uri.edu

Follow this and additional works at: https://digitalcommons.uri.edu/gsofacpubs

Variability approaching the thermal limits can drive diatom community dynamics

Creative Commons License

Variability approaching the thermal limits can drive diatom community dynamics

Stephanie I. Anderson ⬤, Tatiana A. Rynearson ⬤*
Graduate School of Oceanography, University of Rhode Island, Narragansett, Rhode Island

Abstract

Organismal distributions are largely mediated by temperature, suggesting thermal trait variability plays a key role in defining species' niches. We employed a trait-based approach to better understand how inter- and intraspecific thermal trait variability could explain diatom community dynamics using 24 strains from 5 species in the diatom genus *Skeletonema*, isolated from Narragansett Bay (NBay), where this genus can comprise up to 99% of the microplankton. Strain-specific thermal reaction norms were generated using growth rates obtained at temperatures ranging from −2°C to 36°C. Comparison of thermal reaction norms revealed inter- and intraspecific similarities in the thermal optima, but significant differences approaching the thermal limits. Cellular elemental composition was determined for two thermally differentiated species and again, the most variation occurred approaching the thermal limits. To determine the potential impact of interspecific variability on community composition, a species succession model was formulated utilizing each species' empirically determined thermal reaction norm and historical temperature data from NBay. Seasonal succession in the modeled community resembled the timing of species occurrence in the field, but not species' relative abundance. The model correctly predicted the timing of the dominant winter–spring species, *Skeletonema marinoi*, within 0–14 d of its observed peak occurrence in the field. Interspecific variability approaching the thermal limits provides an alternative mechanism for temporal diatom succession, leads to altered cellular elemental composition, and thus has the potential to influence carbon flux and nutrient cycling, suggesting that growth approaching the thermal limits be incorporated into both empirical and modeling efforts in the future.

Temperature is a principal driver of global organismal distributions in both terrestrial (Angilletta 2009; Sunday et al. 2012) and marine (Poloczanska et al. 2013; García Molinos et al. 2015) environments and one of the most important environmental factors shaping microbial composition in the euphotic ocean (Sunagawa et al. 2015). Temperature differentially influences growth and cellular metabolism between organisms (Eppley 1972), which results in thermal niche differentiation among species (Hardin 1960). In microbes, the influence of temperature on growth has been used to characterize the thermal niche of a species, define thermal traits, and predict a species' ability to respond to environmental variability (Litchman et al. 2012). For example, thermal traits have been utilized to interpret species' thermal ranges on a global

scale (Thomas et al. 2012; Boyd et al. 2013). However, the utility of thermal traits remains relatively uncharacterized in terms of their contribution to community dynamics, such as succession and seasonality.

Thermal reaction norms, or performance curves, describe individual or species' responses to a wide range of temperatures and are parameterized by the thermal traits. They peak at the thermal optima and extend to the thermal limits. Between species or individuals, thermal reaction norms can vary along the temperature axis, both in their position horizontally and in their magnitude vertically (Kingsolver 2009); two theoretical examples are depicted in Fig. 1 (adapted from Bolnick et al. 2003). In one example, species display unique growth optima along a thermal gradient that results in clear niche differentiation between species (Fig. 1a). In another example, species display similar thermal optima and niche widths resulting in less niche differentiation (Fig. 1b). While thermal reaction norms can be differentiated in a multitude of ways, greater differentiation, like that depicted in our first example, is readily observed on the global scale as species tend to assort by optima across latitudes (Thomas et al. 2012). However, on regional scales, there are insufficient data to characterize how species structure
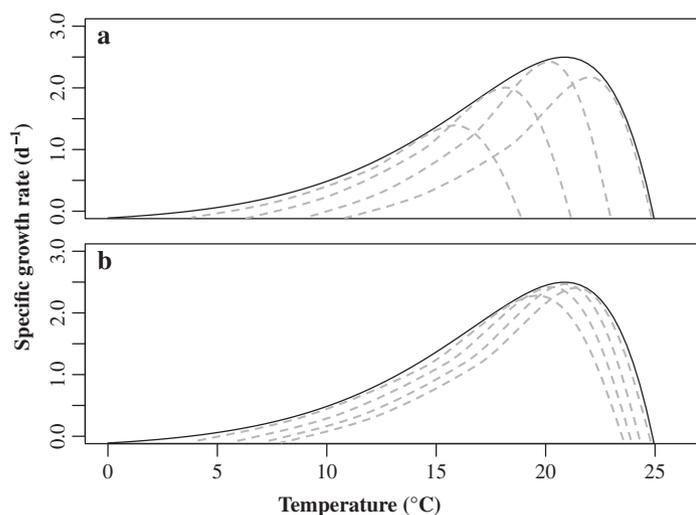
Fig. 1. An illustration depicting two theoretical strategies for defining the thermal niche, both with individual species' niches (dotted lines) and the community niche, comprising all species considered (solid line) (based on Bolnick et al. 2003). Species may constitute the community niche by exhibiting (**a**) nonoverlapping thermal optima and niche widths that span a portion of the community niche or (**b**) wide thermal niches with similar thermal optima that vary primarily at the thermal limits. These illustrations are nonexclusive, serving only as examples of the vast array of possible strategies.

their niche or how the distribution of thermal reaction norms relates to ecological processes such as succession.

This study assessed regional thermal niche partitioning by measuring thermal reaction norms of co-occurring diatom species over a large temperature range, and relating their thermal traits to community dynamics in the field. Diatoms are biogeochemically relevant as they collectively contribute one-fifth of global primary production (Falkowski et al. 1998; Field et al. 1998). Our focal genus, *Skeletonema*, is ecologically important globally (Kooistra et al. 2008; Vargas et al. 2015) and at our study site in Narragansett Bay (NBay), where it generally constitutes over 40% of the phytoplankton >10 μm and as much as 99% of the community during the winter–spring phytoplankton bloom (Karentz and Smayda 1984). *Skeletonema* is an ideal model genus because it comprises several morphologically cryptic, closely related species which occupy different ecological niches (Sarno et al. 2005; Canesi and Rynearson 2016). In addition, *Skeletonema*'s abundance, bloom patterns, and seasonal community composition have been well characterized in NBay (Borkman and Smayda 2009; Canesi and Rynearson 2016), allowing for an unprecedented assessment of the role of thermal traits in environmental niche partitioning. For example, *Skeletonema* species occurrence is strongly correlated with water temperature (Canesi and Rynearson 2016), suggesting species are characterized by differentiated thermal traits.

We employed a trait–based approach to better explain the correlations between diatom community composition and environmental variability. We hypothesized that species subdivided their environmental niches along a temperature gradient leading to differentiated thermal optima, resembling the theoretical example shown in Fig. 1a. This diversification would explain the temporal succession observed in the region and parallel global patterns that link thermal optima to geographic species distribution (Thomas et al. 2012). To test this hypothesis, we addressed the following questions: (1) How have closely related diatom species differentiated their fundamental thermal niche? (2) How does the shape and distribution of thermal reaction norms contribute to species succession in the field? (3) Do differences in species' thermal niches have implications for food web dynamics or biogeochemical cycling? Our findings suggest growth approaching the thermal limits is an important determinant of diatom community dynamics and elemental composition is influenced by species' thermal niches, potentially impacting food web dynamics and biogeochemical cycling.

Methods

Sample collection and cell isolation

We generated a *Skeletonema* culture library consisting of strains from Narragansett Bay (NBay) and the National Center for Marine Algae and Microbiota (NCMA; formerly the CCMP). Strains originating from NBay were isolated from surface whole seawater collected from the NBay Long-Term Plankton Time Series site (41.57° N, 71.39° W) between 2010 and 2016 (https://web.uri.edu/gso/research/plankton/). In situ surface temperatures were recorded using a 6920 Multiparameter sonde (YSI). On dates when *Skeletonema* was abundant (>100 cells ml^{-1}), 16 to 80 single chains were isolated using an SZX16 dissecting microscope (Olympus), washed three times in sterile filtered seawater, and transferred into 1 mL volumes of F/2 media (Guillard 1975). *Skeletonema* isolated from June to September were initially transferred into a 1:10 dilution of F/2 media to avoid nutrient shock and later transferred into F/2. Isolates were cultured at +/− 4°C of their in situ temperature, but later underwent stepwise acclimation to 14°C where they were maintained on a 12:12 LD cycle at 100 μmol photons m^{-2} s^{-1}.

Species identification

Surviving isolates were identified to species using the 28S rDNA sequence. To extract genomic DNA, cultures were centrifuged for 10 min at 12,000×g (Sigma 4 K15 Benchtop Centrifuge) and pellets were resuspended in 0.2 mL Triton X-100 buffer. Samples were incubated for 30 min at 95°C with agitation and then centrifuged for 10 min at 12,000×g (Goldenberger et al. 1995). The 28S rDNA was amplified from the supernatant using a 10 μL reaction mixture containing 1x BIO-X-ACT Short Mix (Bioline), 0.5 μM Skel28SF and Skel28SR primers (Canesi and Rynearson 2016), and 1 μL genomic DNA. The 28S rDNA was amplified in a thermal cycler (Eppendorf AG 22331 Mastercycler) at 94°C for 3 min, followed by 30 cycles of 94°C for 30 s, 60°C for 30 s and 72°C for 1 min, followed by a 10 min extension at 72°C.

All amplicons were sequenced unidirectionally using either Skel28SF or Skel28SR on a 3500XL Genetic Analyzer (Applied Biosystems) at the University of Rhode Island Genomics and Sequencing Center. *Skeletonema* sequences were analyzed using Genomics Workbench software, V9.0.1 (CLC, Qiagen).

A longer portion of the 28S rDNA was amplified and sequenced from isolates initially identified as *Skeletonema tropicum* and *Skeletonema grethae* because these species could not be distinguished using the Skel28SF and Skel28SR primers (Canesi and Rynearson 2016). Genomic DNA from those isolates was extracted using the DNeasy Plant Mini Kit (Qiagen) following manufacturer's instructions. Domains D1–D3 of the 28S rDNA were amplified using primers DIR and D3Ca (Lenaers et al. 1989; Scholin et al. 1994) following the protocol of Godhe et al. (2006). Amplicons were sequenced and analyzed as described previously.

Thermal reaction norm characterization

In total, 24 strains spanning 5 species were chosen for thermal reaction norm characterization (Table S1). Thermal growth response was measured for each strain in temperature-controlled incubators (I-36LLVL Series, Percival Scientific) with a 16:8 LD cycle at the optimal growth irradiance of 150 μmol photons m^{-2} s^{-1} (Supplemental Methods, Fig. S1). Experimental temperatures were characteristic of NBay ($-2°$C to 25°C) and higher (up to 36°C), and included 1°C increments approaching the thermal limits to accurately capture the limits (Table S2, Rynearson 2019*a*). Strains acclimated to each temperature for ≥8 generations prior to the onset of the experiment. Daily measurements of in vivo Chlorophyll *a* fluorescence were recorded using a 10-AU Fluorometer (Turner Designs) or Microplate Reader (Spectramax M Series, Molecular Devices) for test tubes or well plates, respectively. No significant differences were detected between growth rates obtained using the two instruments (Supplemental Methods, Fig. S2). Following Boyd et al. (2013) and Brand et al. (1981), the specific growth rate (Gotelli 1995) for each strain at each temperature was calculated using a minimum of three serial replicates conducted after acclimation to the treatment temperature. Statistical analyses were utilized to ensure fit and similarity of regression (R^2, F statistic, F-test; Zar 1996) among replicate growth rates for each strain, at each temperature. Additional growth curves were measured until at least three consecutive trials produced growth rates that were not significantly different (Boyd et al. 2013). This approach ensures strains have acclimated to the treatment temperature, but has the potential to underestimate uncertainty in growth measurements. The standard error and coefficient of variation (CV) were calculated for triplicate growth curves, for each strain, at each temperature.

Thermal reaction norms were generated for each strain using experimental replicate growth data and the following thermal tolerance function adapted from Norberg (2004):

$$\mu(T) = ae^{bT}\left[1 - \left(\frac{T-z}{\frac{w}{2}}\right)^2\right] \qquad (1)$$

where μ is the specific growth rate as a function of temperature T, w is the thermal niche width, z is the maximum of the quadratic expression, and a and b are species-specific parameters. Coefficients for model fit were determined using nonlinear least squares estimations of growth data in R 3.4.1 (R Core Team 2017) and 95% confidence intervals were estimated for each parameter using the nlstools package in R (Baty et al. 2015).

Thermal traits were then estimated for each strain for which a reaction norm could be fit (≥5 temperatures examined). This allowed enough growth-temperature coverage to be confident in resulting trait estimations. The *x*-intercepts of each strain-fitted reaction norm were characterized as the thermal minima and maxima. When the minima fell below the freezing point of seawater ($-2°$C), they were adjusted to $-2°$C, as *Skeletonema* is not known to inhabit sea ice. Niche widths (the difference between the maxima and minima), and the thermal optima (the reaction norm maxima) were assessed. Standard errors in modeled thermal traits were estimated by parametric bootstrapping with 10,000 samples (Supplemental methods). Species trait values were assessed for homogeneity of variance using Levene's Test (car package in R, Fox and Weisberg 2011). An analysis of variance (ANOVA) and a Tukey's Multiple Comparison test (DTK package in R, Lau 2013) were performed to test for differences between species' trait values (Zar 1996).

Carbon and nitrogen composition analysis

The influence of temperature on elemental composition was examined in two species, *Skeletonema marinoi* and *Skeletonema pseudocostatum*. These species were characterized by different seasonal occurrences (Canesi and Rynearson 2016), large sample sizes isolated at diverse temperatures, and significantly different thermal traits, determined during the course of this study. Experimental temperatures were selected based on the thermal minimum and maximum for each strain and included an approximate thermal optimum of 22°C. Cultures were maintained in temperature-controlled incubators and their growth was monitored as described previously.

Cell concentrations were determined for each strain at each temperature immediately before harvesting using 1 mL Sedgewick counting cells (Structure Probe) and an Eclipse E800 microscope (Nikon). A minimum of 1000 cells were counted. Linear measurements of height and diameter were recorded for 30 live cells from each strain and used to calculate cell volume using the volume of a cylinder (Montagnes and Franklin 2001).

Prior to harvesting, GF/F filters and 20 mL glass scintillation vials were precombusted at 450°C for 24 h. From each culture and during exponential growth phase, ≥1 × 10^7 cells were filtered in triplicate onto precombusted 25-mm GF/F filters, and rinsed with 10 mL F/2 media. Blanks were made to
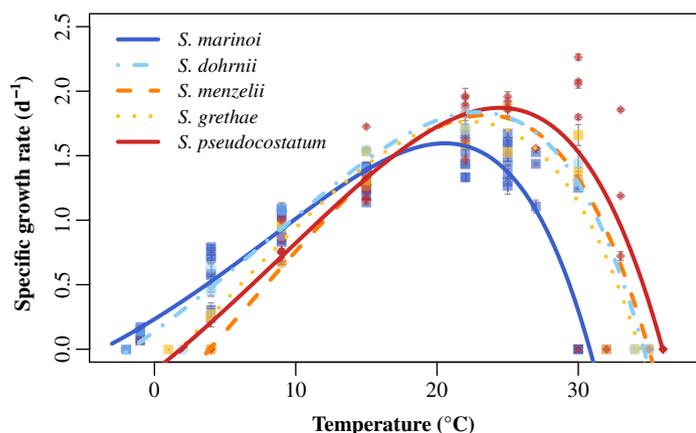
Fig. 2. Thermal response curves for each species examined. Curves were constructed from growth data obtained from multiple strains and parameterized using nonlinear least square estimations (Thomas et al., 2012). Points signify the mean growth rates for each strain and error bars denote standard error from triplicate growth trials. *S. marinoi* displayed the lowest thermal minimum (*n* = 9), while *S. dohrnii* (*n* = 3), *S. menzelii* (*n* = 1), *S. grethae* (*n* = 3), and *S. pseudocostatum* (*n* = 8) were characterized by higher thermal maxima and a greater average growth rates at high temperatures.

correct for any elemental contribution from filters or media. All filters were then placed in glass scintillation vials and stored at −80°C until further analysis.

Immediately prior to analysis, filters were dried at 60°C for 24 h. The mass of the filter, total volume filtered, and cell counts were utilized to determine the number of cells analyzed. Elemental composition was assessed on an elemental analyzer (CE-440, Exeter Analytical), and carbon and nitrogen content per cell, carbon density, and carbon to nitrogen ratios

(C:N) were calculated for each strain. For each variable, the CV was determined for each species, and species' elemental composition was compared using ANOVA.

Construction of a species succession model

A species succession model was developed to determine how thermal trait variability could impact *Skeletonema* community composition in NBay. First, a thermal reaction norm was generated for each species by fitting species-specific parameters (Eq. 1) to growth data from all strains of each species, using nonlinear estimations. By taking the mean for each species, we eliminated biases due to differences in sample size, but did not account for intraspecific variability. Second, a nonlinear regression was fit to NBay weekly surface temperature data from 2008 to 2012 (https://web.uri.edu/gso/research/plankton/), so the modeled *Skeletonema* community could be compared with field observations (Canesi and Rynearson 2016), with an additional year for model stabilization. Due to uneven sampling time steps, temperature data was interpolated across the time frame using a nonparametric approach (Fig. S3a; R Core Team 2017). Each species' growth rates over time were then estimated using a modified version of Eq. 1, in which μ was instead a function of temperature at time of year $\mu[T(t)]$ (Fig. S3b).

A simulation to determine the influence of thermal trait variability on *Skeletonema* community composition in NBay began with equal proportions of each species and operated under the assumptions that species (1) received experimental growth conditions (i.e., optimal light and nutrient replete conditions) and (2) were maintained in exponential growth. The number of cells per liter (*N*) for each species was calculated using an exponential growth model according to Eq. 2 (Cáceres et al. 2013), where the population size (*N*) at a given
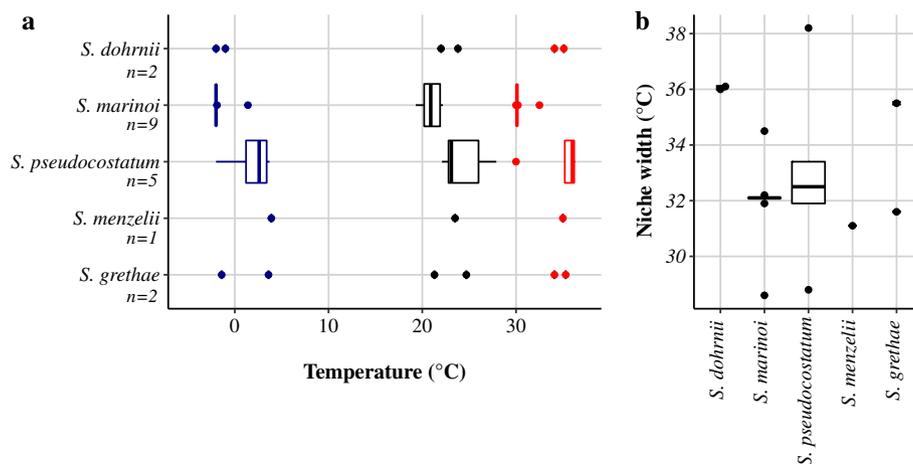

Fig. 3. Thermal trait variability in *Skeletonema* species. The thermal minimum (**a**, blue), thermal optimum (**a**, black), thermal maximum (**a**, red), and niche width (**b**) were estimated for each strain based on the model by Norberg (2004). Traits are only shown for strains that had sufficient data to fit a Norberg curve (19 of 24). Boxplots are shown for species with ≥3 strains and display the median and lower and upper quartiles of trait distributions within each species, with points representing trait outliers. For species with <3 strains assessed, traits are shown as points and error bars denote the standard error in model fit estimated through parametric bootstrapping (not visible if smaller than symbol). *S. dohrnii* had the greatest niche width of the species examined. Species displayed similar thermal optima, but were characterized by significantly different thermal minima (ANOVA, *p* = 0.01).

time of year (t) grows according to the difference between the specific growth rate at that time of year (μ_t; determined from the modified Eq. 1) and the grazing rate per day (g). The grazing rate was then modeled to follow a saturating response (Eq. 3) termed the Ivlev response (Ivlev 1945), which has been observed previously in *Skeletonema* grazers (Deason 1980) and depicts grazing that increases with the concentration of available prey.

$$N(t) = N_{(t-1)}\, e^{[\mu_t - g(N)]\delta t} \tag{2}$$

$$g(N) = R_m\left(1 - e^{-\lambda N}\right) \tag{3}$$

Grazing intensifies according to the rate of saturation (λ) until it reaches a maximum grazing rate (R_m). Here, R_m in NBay was estimated to be 1.8 d^{-1} based on Lawrence and Menden-Deuer (2012). λ was adjusted until resulting *Skeletonema* concentrations were proportionate to those measured in NBay (https://web.uri.edu/gso/research/plankton/), which resulted in a λ of 1×10^{-5} cell/L^{-1}. A time step (δt) was also included to control the rate at which the simulation progressed. The simulation was executed for 1 yr to allow for model stabilization and then it was evaluated for its ability to explain observed *Skeletonema* communities in the field (Canesi and Rynearson 2016). Cross-correlations of modeled and interpolated field communities obtained from high-throughput DNA sequencing (Canesi and Rynearson 2016) were utilized to assess whether the model accurately predicted species' bloom timing, and linear models were employed to determine if the model could account for variability in observed field communities (R Core Team 2017). Figures were plotted using the R package ggplot2 (Wickham 2016).

Results

Culture library

Between March 2015 and July 2016, 184 *Skeletonema* strains were isolated from NBay, successfully cultured, and their 28S rDNA sequenced. Four species were identified within the culture library, with 92.4% classified as *S. marinoi* (*S.ma.*). Seven strains of *S. marinoi* isolated at a diverse range of temperatures (−0.94°C to 19.81°C) were chosen for physiological experiments (Table S1). All newly isolated strains characterized as *Skeletonema dohrnii* (*S.d.*), *S. pseudocostatum* (*S.p.*), and *S. grethae* (*S.g.*), as well as all strains obtained from NCMA were incorporated into the physiological experiments. *Skeletonema menzelii* (*S.me*) was not found in the culture library, but an NCMA strain was included in the study for its ecological relevance (Canesi and Rynearson 2016), leading to a total of 24 strains.

Thermal trait variability

Thermal reaction norms could be fit for 19 of the 24 strains examined, allowing for trait estimations and comparisons. There was substantial overlap in the thermal response curves of the five *Skeletonema* species examined (Fig. 2). Thermal optima were only significantly different between two species,

S. marinoi and *S. pseudocostatum* (Tukey's, $p = 0.02$, Fig. 3a). Niche widths were also not significantly different among species (ANOVA, $p > 0.1$, Fig. 3b). While the mean niche widths differed between species by as much as 5°C (Fig. 3b), intraspecific variation was great (i.e., *S.g.* and *S.p.*, $\sigma^2 > 10$°C), resulting in statistical nonsignificance.

Variability among species was observed at the thermal limits. The thermal minima were significantly different among species (ANOVA, $p = 0.01$). For several strains, the exact thermal minima could not be determined before freezing occurred, suggesting a high capacity for cold tolerance. In contrast, thermal maxima were not differentiated between species (ANOVA, $p > 0.9$) with the exception of *S. marinoi*. *S. marinoi* had a maximum that was significantly different from all species examined, except *S. menzelii* (Tukey's, *S.g.*, *S.p.*, *S.d.*: $p < 0.05$). All species
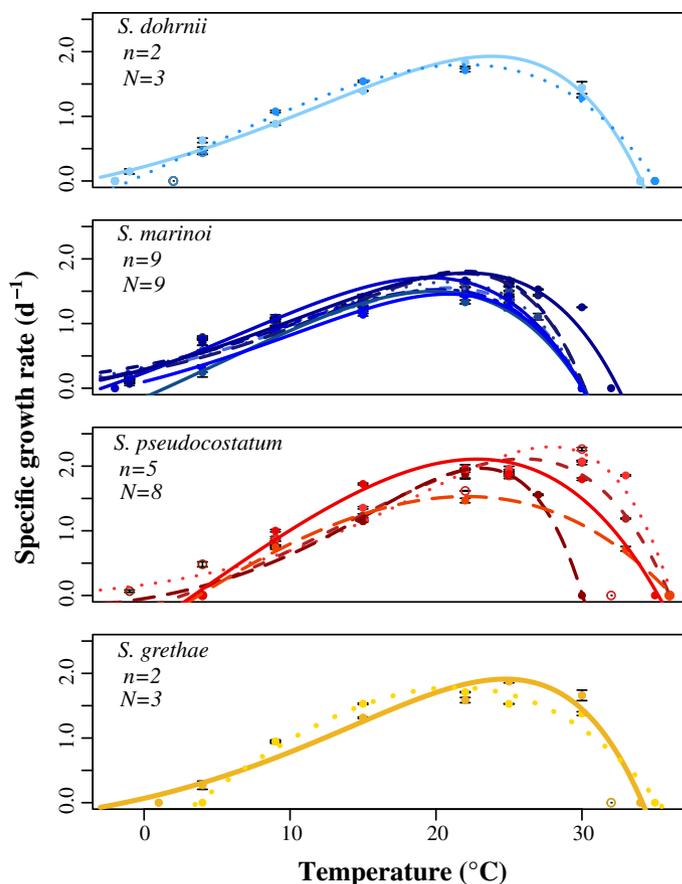

Fig. 4. Intraspecific variation in thermal response curves generally increased approaching the thermal limits. Response curves were fit to mean growth rates for each strain (points) using nonlinear least square estimations (Thomas et al., 2012). Each panel displays strains from a single species. *S. menzelii* has been omitted from this intraspecific analysis as only one strain was examined. The number of strains examined for which a response curve could be fit (≥5 temperatures assessed, *n*) may differ from the total number of strains examined (*N* and open circles), if there were strains with insufficient data. Error bars denote standard error from triplicate growth trials.

displayed maxima of ≥30°C, which far surpasses temperatures recorded in NBay (https://web.uri.edu/gso/research/plankton/).

Intraspecific variation in the thermal traits mirrored interspecific variation, with the greatest variation occurring at the thermal limits. Thermal minima and maxima ranged by as much as 6°C within each species (Fig. 4). Growth rates also varied approaching the thermal limits. While growth was variable throughout the temperature range examined (Table S2, Rynearson 2019*a*), the greatest divergence within species was at the thermal extremes, with growth rates among strains that differed by as much 1 d^{-1} (Fig. 4).

Additional assessments of intraspecific variability were conducted using species with the largest sample sizes, *S. marinoi* (*n* = 9) and *S. pseudocostatum* (*n* = 8). For both species, the growth rate CV was found to be greatest approaching the thermal limits and least at the thermal optimum, resulting in a hyperbolic trend (Fig. 5a). For strains with a known SST at time of isolation (*S.ma. n* = 8, *S.p. n* = 7; Table S1), temperature was utilized to assess whether there could be an evolutionary component to the thermal variation observed between strains. There were no significant correlations between temperature at isolation and growth rate at either the thermal optima (Fig. 5b) or at temperatures approaching the thermal limits (Fig. S4).

Carbon and nitrogen composition analysis

The influence of temperature on elemental composition was compared for a subset of strains from a species with frequent occurrence in winter–spring, *S. marinoi* (*n* = 3), and one with frequent occurrence in summer–autumn, *S. pseudocostatum* (*n* = 4; Canesi and Rynearson 2016). Trends in carbon density with temperature were opposing between species, though only significant for *S. pseudocostatum* (Fig. 6a; *S. ma.*: *r* = 0.6, *p* = 0.08; *S.p.*: *r* = −0.6, *p* = 0.03), with the greatest differences between species at their respective thermal minima (ANOVA, *p* < 0.01). However, there were no significant trends in nitrogen density with temperature for either species (*S.ma and S.p. R^2* < 0.1, *p* > 0.5; Fig. 6b). This resulted in carbon to nitrogen ratios (C:N) that followed a similar relationship as that of carbon density. At each species' thermal minimum, *S. marinoi* and *S. pseudocostatum* were characterized by a significant, two-fold difference in C:N (ANOVA, *p* < 0.01, Fig. 6c). However, at the thermal optima (22°C), both species had C:N in Redfield proportions, with *S. marinoi* and *S. pseudocostatum* exhibiting average C:N of 7.4 and 6.4, respectively. There was a significant correlation between C:N and growth rate in *S. marinoi* (*r* = 0.7, *p* = 0.02), but not *S. pseudocostatum* (*r* = −0.6, *p* = 0.06; Fig. 6d). For *S. marinoi*, molar nitrogen per cell was significantly correlated with cell volume (*r* = 0.8, *p* = 0.01), and the minimum cell volume, and thus elemental content, occurred at the thermal optimum (Fig. S5). Intraspecific variation in C:N for *S. marinoi* and *S. pseudocostatum* was observed, with the C:N CV as high as 18%. Maximum intraspecific differences occurred near the thermal minima (Table S3, Rynearson 2019*b*).

Species succession

A theoretical model was formulated to evaluate the potential influence of thermal growth variability on *Skeletonema* community dynamics. To construct this, species' thermal reaction norms were employed in conjunction with NBay temperature data from the time series (https://web.uri.edu/gso/research/plankton/). Species' temperature-growth data were mapped to weekly SST data from NBay to better understand how species' growth rates could vary over time (Fig. S3). Small differences in the thermal minima and maxima between species, as well as varied growth rates, resulted in seasonal species succession in the modeled *Skeletonema* community (Fig. 7a). The model predicted a shift from a community dominated by *S. marinoi* and *S. dohrnii* to one more evenly composed of all species in the summer months, which generally mirrors that seen in the field (Fig. 7b). Overall, the model did not accurately replicate the percent composition, magnitude or variability for each species in the field (Fig. 7b, Table S6). However, there was a positive correlation in the timing of peak percent abundance for 4 of 5 species (Fig. S6, Table S6). The model was especially effective at predicting the timing of maximum percent abundance in *S. marinoi*, as the predicted and actual values were only offset by an average of 8 d (mean correlation from 2008 to 2011 = 0.85). When each year was considered separately, the model predicted the timing of maximum percent abundance exactly for 2010 (cross correlation at lag 0 d = 0.917), and was offset from field observations by 15 d in 2009 (cross correlation at lag −15 d = 0.906). In comparison, the predicted peaks for *S. menzelii*, *S. grethae*, and *S. pseudocostatum* were offset from field data by 1–2 months.

Discussion

Several studies have previously utilized thermal reaction norms from literature compilations (Thomas et al. 2012) or community wide studies (Boyd et al. 2013) to make inferences about environmental niche partitioning. These approaches afford the large sample sizes necessary to draw conclusions about thermal traits across habitats. We adapted these methodologies in order to understand the role of thermal niche partitioning on species succession at regional scales, and generated a representative assortment of thermal reaction norms from species that co-occur in a single area. We lessened the likelihood of introducing method biases by evaluating strains in one comprehensive common garden study, where experimental conditions could be standardized. In addition, the majority of our strains were isolated within a year of experimentation, which is relevant given that microbes have short generation times, allowing them to evolve quickly to culturing conditions, potentially influencing thermal traits (Bennett et al. 1992; Brennan et al. 2017). Furthermore, by including multiple strains from individual species in this study, we were able to examine thermal trait
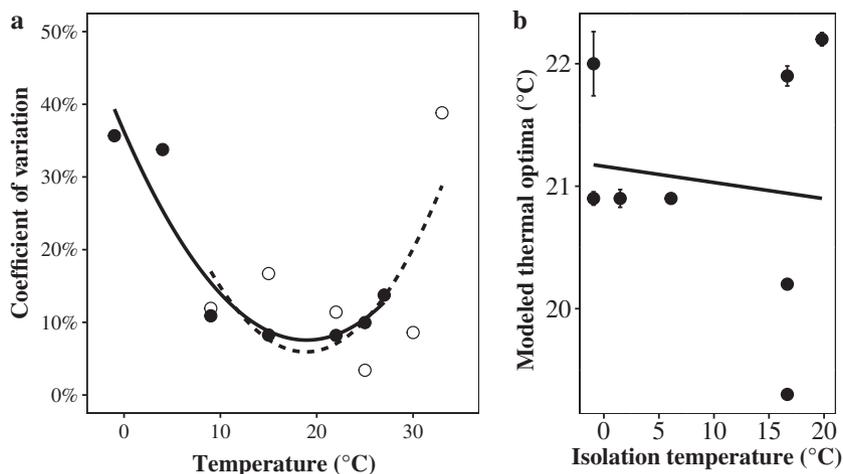
Fig. 5. Growth variability within species increases toward the thermal limits. (**a**) The growth rate coefficient of variation (CV) was calculated for *S. marinoi* (black, solid line) and *S. pseudocostatum* (white, dashed line) at each temperature where at least two strains exhibited positive growth. The CV between strains (points) displayed a quadratic trend for each species (lines), signifying increasing growth variability toward the thermal extremes. (**b**) The thermal optima for *n* = eight strains of *S. marinoi*, estimated using strain-fitted reaction norms, were not related to sea surface temperature at time of isolation ($R^2 < 0.2$). Error bars denote the standard error in modeled thermal optima derived from parametric bootstrapping.
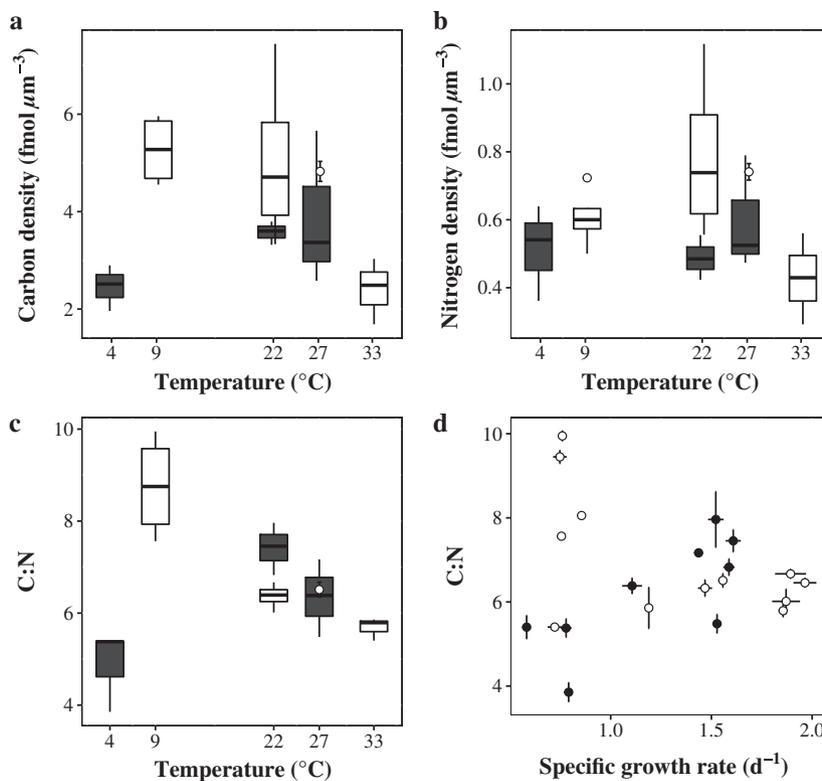

Fig. 6. Species elemental composition diverged at the thermal limits. (**a**) The carbon density of *S. marinoi* (gray, *n* = 3) was significantly lower than *S. pseudocostatum* (white, *n* = 4) at temperatures approaching species thermal minima, 4°C and 9°C respectively. (**b**) Nitrogen density did not vary significantly between temperature treatments for either species (Tukey's, *p* > 0.1) resulting in (**c**) a C:N resembling carbon density trends, with the greatest differences again observed at the thermal minima. Some variability in C:N may have resulted from differences in growth (**d**) as C:N was correlated with specific growth rate for both species (*S.m. r* = 0.7, *p* = 0.02; *S.p. r* = −0.6, *p* = 0.06). Boxplots are shown for temperatures at which ≥3 strains were examined and display the median, and lower and upper quartiles of elemental distributions within each species. Points depict mean values for triplicate samples and error bars display the standard error.

variation both within and between species, allowing us to draw conclusions about how the structure and distribution of species' reaction norms influence diatom community dynamics.

Variability at the thermal limits

The distribution of thermal reaction norms among *Skeletonema* species across the thermal gradient was unexpected. Given their seasonal occurrence in NBay, we hypothesized that each species would have a thermal optimum corresponding to the temperature at which it was most commonly found in the environment (like that shown in Fig. 1a). In NBay, for example, *S. marinoi* is the dominant *Skeletonema* species in the winter and spring, when it can comprise 99% of the phytoplankton community (Canesi and Rynearson 2016). We hypothesized that *S. marinoi* was a thermal specialist with a preference for, or optimum at, winter–spring temperatures (<10°C); analogous to *S. marinoi* salinity specialists (Sjöqvist et al. 2015). However, our reaction norm characterizations revealed that *Skeletonema* species were generally not differentiated by their thermal optima, as observed in *Skeletonema* species isolated from the NW Pacific (Kaeriyama et al. 2011). Instead, we found NBay *Skeletonema* species to possess wide thermal niches, characteristic of eurythermal species (Karentz and Smayda 1984), that were distinguished by differences at the thermal limits, bearing resemblance to the diagram in Fig. 1b. For example, unlike its congeners, *S. marinoi* showed positive growth up to the freezing point of seawater (−2°C), which may explain its dominance during winter and spring (Canesi and Rynearson 2016), despite its relatively slow

growth rates at these temperatures. Comparably, the four species present in summer (*S. menzelli*, *S. grethae*, *S. pseudocostatum*, and *S. dohrnii*) were differentiated from *S. marinoi* by significantly higher thermal maxima. These findings are consistent with other NBay species which similarly have a temperature of occurrence that differs from, and is typically below, their thermal optima (Karentz and Smayda 1984).

It has been suggested that adaptation to thermal extremes, such as near-freezing water, may entail a trade-off to performance at moderate temperatures (Angilletta 2009). This idea stems from the Principle of Allocation (Levins 1968), which proposes that advantages are only obtained at a cost to other functionality. Here, we observed that *S. marinoi* had the highest growth rates at the lowest temperatures compared with the other species examined, but the slowest growth rates at the thermal optimum. *S. marinoi*'s realized niche, defined by the species' ability to thrive in the range of temperatures characteristic of the region (−2°C to 25°C), was also the greatest of the species examined. This trade-off between performances at moderate temperatures in favor of extreme temperatures resulted in a depressed thermal reaction norm, but a wider realized niche for *S. marinoi*, which may be more indicative of a thermal generalist (Huey and Hertz 1984), contrary to our initial hypothesis of winter specialization. These results illustrate how species may develop thermal strategies through trade-offs and variation at the thermal limits, in addition to differentiation at the thermal optima.

The shape of thermal reaction norms in this set of closely related *Skeletonema* species may also be constrained by their presumably similar genetic background, which may influence
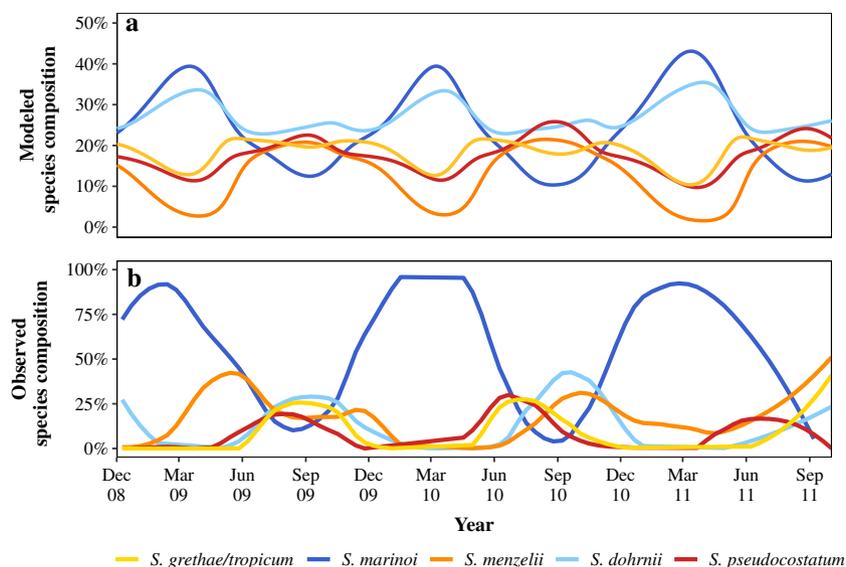

Fig. 7. Comparison between (**a**) the modeled *Skeletonema* community over time and (**b**) an observed *Skeletonema* community from December 2008 to October 2011 (Canesi and Rynearson 2016) shows a strong correlation in the timing of peak occurrence for each species. Simulation (**a**) utilizes experimental growth data, NBay weekly temperature data from the NBay long-term plankton time series, and the Ivlev (1945) model for grazing to depict how thermal trait variability could influence community composition in the field. Note that the *y*-axis scales differ to allow for comparison in the timing, rather than magnitude, of peak abundance for different species.

how thermal reaction norms can change in response to natural selection. In terrestrial organisms, the evolutionary potential of the thermal maxima is predominately regulated by phylogeny rather than temperature, and this is reversed at the thermal minima (Diamond and Chick 2018). However, in diatoms, the evolutionary potential of thermal traits remains largely unknown (reviewed in Litchman et al. 2012). Evidence from a single species suggests that thermal adaptation may be quite rapid in diatoms (O'Donnell et al. 2018; Schaum et al. 2018) with the thermal optima being more susceptible than the thermal limits to warming (O'Donnell et al. 2018). However, these findings are not consistent across the phytoplankton (Listmann et al. 2016; Padfield et al. 2016). Studies are needed to compare the evolutionary response of thermal traits in closely vs. distantly related diatom taxa.

Variability drives species succession

To examine how variation at the thermal limits might influence species succession, we developed a model that incorporated just three terms: the measured thermal reaction norms, NBay surface water temperatures, and density-dependent grazing. The model correctly predicted species succession from a less diverse spring community to a more diverse summer community. It also accurately forecasted the occurrence of four out of five *Skeletonema* species to within 2 months of their actual dominance in the field. For *S. marinoi*, the model predicted the exact day the species would be most dominant in the community for one of the years assessed, and was within 2 weeks across the 3-year model-field data comparison. However, the model could not accurately predict species' absolute or percent abundance, only the timing at which maximum abundance would occur. This could have resulted from additional factors not accounted for in our model, such as nutrient availability, salinity, or grazing; all of which vary seasonally in the study region (Windecker 2010; Lawrence and Menden-Deuer 2012). Additionally, the species' reaction norms used in this simple model may not fully characterize the high diversity present in diatom populations (Rynearson and Armbrust 2005), which could alter predictions of species' seasonal occurrences. Despite these limitations, the model's ability to replicate field observations of a species rich summer–fall community, a less diverse winter–spring community, and yearly variations in the timing of species succession (Canesi and Rynearson 2016), support temperature as a strong predictor of temporal species composition.

There were some additional discrepancies between the modeled and measured *Skeletonema* composition. For example, the model predicted *S. dohrnii* to occur during winter, when it is typically sparse (Canesi and Rynearson 2016). Differences in *S. dohrnii* composition may result from direct or indirect competition with other species. For example, *S. marinoi* may be a stronger competitor in spring due to the species' seasonal polyunsaturated aldehyde production, which hinders predators (Miralto et al. 1999; Taylor et al. 2009). If this proved to be a contributing factor in determining species composition, a preferential grazing model

would have been more fitting than our density-dependent equation, which assumes no preferential grazing among species.

An important point is that species succession in the model was predicted as a result of differentiation approaching the thermal limits rather than at the thermal optima. This can be concluded based on the occurrence of each species relative to their thermal traits. For example, only *S. marinoi* and *S. dohrnii* are predicted to be present at cooler temperatures and this results from their significantly lower thermal minima, which equips them with greater growth rates at these temperatures. Community succession then occurs when all species are present, but before any have reached their optima. While it should be noted that *S. marinoi* is ultimately outcompeted due to its relatively lower growth rate at its thermal optimum, the reason for which it is ever dominant lies in its lower thermal minimum. This signifies that even species with similar thermal optima can have differentiated seasonal dynamics based on their thermal minima; a conclusion which can be logically reasoned, but to our knowledge, has not been shown previously.

Most current models of species distribution use modeled estimations of the thermal limits (García Molinos et al. 2015; Barton et al. 2016) or primarily focus on differences at the thermal optima (Thomas et al. 2012). While these methods provide valuable insight into global ecological structuring, they cannot as easily be applied to regions where genera with nondifferentiated optima, like *Skeletonema*, dominate the seascape. By incorporating empirically derived thermal limits into phytoplankton species distribution models, one may be able to make predictions about phytoplankton distribution in relation to time as well as space. This added complexity would likely provide valuable insights into phytoplankton community dynamics.

Biogeochemical implications of variation approaching the thermal limits

Shifts in elemental composition across the thermal reaction norm and between species can influence biogeochemical cycling. The two species examined, *S. marinoi* and *S. pseudocostatum*, differed in their thermal traits, with significant differences in thermal minima, maxima, and optima, making them ideal candidates for stoichiometric comparisons (Martiny et al. 2016). At their thermal minima, the two species diverged in carbon density and C:N suggesting they have developed different strategies for coping with the stress of low temperatures. For example, *S. marinoi* had a lower C:N than *S. pseudocostatum* at its respective thermal minimum, potentially indicating higher cellular protein content, which may contribute to positive growth at low temperatures (Geider and La Roche 2002; Yvon-Durocher et al. 2015; Kirchman 2016). An explanation for the relationship between C:N and temperature has not yet been established, as thermal trends in C:N vary significantly from species to species (Thompson et al. 1992; Berges et al. 2002). However, it has been proposed that C:N can deviate from Redfield proportions under low growth conditions (Goldman et al. 1979; Goldman 1986), which is both consistent with our observations and may provide

some insight into the temperature C:N relationship. Lower elemental content may also be characteristic of species with higher thermal optima, such as *S. pseudocostatum* (Barton and Yvon-Durocher 2019). Thus, the impact of temperature on cellular composition may result from several metabolic strategies occurring simultaneously to cope with thermal extremes.

The implications of physiological variation at the thermal limits extend to biogeochemical cycles and trophic dynamics. Our finding that species exhibit varied elemental composition indicates that temperature-driven shifts in species composition alter the elemental makeup of primary producers. For example, a shift from *S. marinoi* to *S. pseudocostatum* with warmer temperatures would be accompanied by a shift to higher C:N. This is consistent with observed seasonal patterns that find higher C:N in the summer and fall (Frigstad et al. 2011; reviewed in Moreno and Martiny 2018). Such changes to species and their stoichiometry correspond to shifts in nutritional quality for higher tropic levels (Sterner and Elser 2002). For example, in zooplankton, eating poor quality prey (high C:N) decreases assimilation efficiency (Sailley et al. 2015), which can affect growth (reviewed in Finkel et al. 2010). Decreased assimilation efficiency in zooplankton can limit nutrient regeneration, altering the composition of particulate matter in the water column and decreasing primary production (Finkel et al. 2010). Thus, shifts in species composition have broad implications for carbon and nutrient cycling in marine environments.

Terrestrial studies have long used the niche space to forecast how species ranges may be altered by temperature (Kearney 2009), but oceanographic models are still largely limited in their predictive capacity due to a lack of experimental data regarding the thermal limits (García Molinos et al. 2015). While studies have been able to define the niche space using other metrics, such as phytoplankton abundance data, to predict future geographic shifts (Barton et al. 2016), our study indicates the value in experimentally deriving the thermal limits. Identifying the thermal maxima can reveal a species' warming tolerance and thermal safety margin (Deutsch et al. 2008) and categorizing the thermal minima is relevant for species that rely on a competitive advantage in colder climates, like *S. marinoi*. For example, at our study site in NBay, winter sea surface temperatures have increased by 2.2°C since the 1960s (Nixon et al. 2009), which has led to a shift in *Skeletonema* bloom dynamics, from the major yearly bloom typically occurring in spring, to one that is now increasingly transpiring in summer and autumn (Borkman and Smayda 2009). This shift may have resulted from a decrease in competitive advantage for the dominant cold-water species, *S. marinoi* (Canesi and Rynearson 2016). It has also been argued that shifts in NBay bloom timing and species composition are impacting higher trophic levels in NBay (Nixon et al. 2009). Our finding that *Skeletonema* species possess varied elemental stoichiometry provides one mechanism to explain this phenomenon.

Intraspecific variation

The patterns of thermal variability found within species paralleled those observed between species, with the greatest intraspecific variation measured at the thermal limits. For example, approaching the thermal minima, strains of *S. marinoi* had growth rates that varied by as much as 1 d^{-1}, or nearly 1.5 doublings d^{-1}. Strains of *S. pseudocostatum* expressed diverse thermal maxima, resulting in large coefficients of variation at the thermal limits (45%) but not at the thermal optima (2%). Examples of intraspecific variation at the thermal limits have been noted in other phytoplankton species, like *T. rotula* (Whittaker et al. 2012; Boyd et al. 2013). This phenomenon has also been well characterized in terrestrial organisms, where performance rapidly decreases away from the optimum, but not always at a similar rate among individuals (reviewed in Dowd et al. 2015). Our findings highlight the high degree of variability that exists within the species' niche, which can only be captured through the characterization of multiple strains within a species. The level of intraspecific variation captured here suggests that evaluation and extrapolation of single strains to represent species with high levels of physiological diversity should be conducted with care, as they may only represent a fraction of the niche that a species occupies.

Conclusion

Several models have been formulated to explain how organisms structure their environmental niche, including those presented in Fig. 1 (Bolnick et al. 2003). Often, species are thought to differentiate their growth optima along environmental gradients (Fig. 1a, Godhe and Rynearson 2017), resulting in species succession with each conditional shift. Our results suggest that variation at the thermal limits can also influence community structure and provide an alternate mechanism for species succession. The species examined in this study were characterized by wide thermal niches, with similar optima, but significant divergence at the thermal limits—more closely aligning with the second theoretical model in Bolnick et al. (Fig. 1b). Incorporation of thermal limits into models of phytoplankton community structure as well as variable elemental compositions should enable more precise projections of how phytoplankton communities may shift with future temperature fluctuations. By relating variability at the thermal limits to temporal community composition in the field, our study identified an alternative, and often overlooked, aspect of phytoplankton species' niche space.

References

Angilletta, M. J. 2009. Thermal adaptation: A theoretical and empirical synthesis. Oxford Univ. Press.

Barton, A. D., A. J. Irwin, Z. V. Finkel, and C. A. Stock. 2016. Anthropogenic climate change drives shift and shuffle in North Atlantic phytoplankton communities. Proc. Natl. Acad. Sci. USA **113**: 2964–2969. doi:10.1073/pnas.1519080113

Barton, S., and G. Yvon-Durocher. 2019. Quantifying the temperature dependence of growth rate in marine phytoplankton within and across species. Limnol. Oceanogr. **64**: 2081–2091. doi:10.1002/lno.11170

Baty, F., C. Ritz, S. Charles, M. Brutsche, J.-P. Flandrois, and M.-L. Delignette-Muller. 2015. A toolbox for nonlinear regression in {R}: The package {nlstools}. J. Stat. Softw. **66**: 1–21.

Bennett, A. F., R. E. Lenski, and J. E. Mittler. 1992. Evolutionary adaptation to temperature. I. Fitness responses of *Escherichia coli* to changes in its thermal environment. Evolution (N. Y). **46**: 16–30. http://www.jstor.org/stable/2409801

Berges, J. A., D. E. Varela, and P. J. Harrison. 2002. Effects of temperature on growth rate, cell composition and nitrogen metabolism in the marine diatom *Thalassiosira pseudonana* (Bacillariophyceae). Mar. Ecol. Prog. Ser. **225**: 139–146. doi:10.3354/meps225139

Bolnick, D. I., R. Svanbäck, J. a. Fordyce, L. H. Yang, J. M. Davis, C. D. Hulsey, and M. L. Forister. 2003. The ecology of individuals: Incidence and implications of individual specialization. Am. Nat. **161**: 1–28. doi:10.1086/343878

Borkman, D. G., and T. Smayda. 2009. Multidecadal (1959-1997) changes in Skeletonema abundance and seasonal bloom patterns in Narragansett Bay, Rhode Island. USA. J. Sea Res. **61**: 84–94. doi:10.1016/j.seares.2008.10.004

Boyd, P. W., and others 2013. Marine phytoplankton temperature versus growth responses from polar to tropical waters—outcome of a scientific community-wide study. PLoS One **8**: e63091. doi:10.1371/journal.pone.0063091

Brand, L. E., R. L. Guillard, and L. S. Murphy. 1981. A method for the rapid and precise determination of acclimated phytoplankton reproductions rates. J. Plankton Res. **3**: 193–201. doi:10.1093/plankt/3.2.193

Brennan, G. L., N. Colegrave, and S. Collins. 2017. Evolutionary consequences of multidriver environmental change in an aquatic primary producer. Proc. Natl. Acad. Sci. USA **114**: 9930–9935. doi:10.1073/pnas.1703375114

Cáceres, C., F. G. Taboada, J. Höfer, and R. Anadón. 2013. Phytoplankton growth and microzooplankton grazing in the subtropical Northeast Atlantic D.L. Kirchman [ed.]. PLoS One **8**: e69159. doi:10.1371/journal.pone.0069159

Canesi, K., and T. Rynearson. 2016. Temporal variation of Skeletonema community composition from a long-term time series in Narragansett Bay identified using high-throughput DNA sequencing. Mar. Ecol. Prog. Ser. **556**: 1–16. doi:10.3354/meps11843

Deason, E. E. 1980. Grazing of *Acartia hudsonica* (A. clausi) on *Skeletonema costatum* in Narragansett Bay (USA): Influence of food concentration and temperature. Mar. Biol. **60**: 101–113. doi:10.1007/BF00389153

Deutsch, C. A., J. J. Tewksbury, R. B. Huey, K. S. Sheldon, C. K. Ghalambor, D. C. Haak, and P. R. Martin. 2008. Impacts of climate warming on terrestrial ectotherms across latitude. Proc. Natl. Acad. Sci. USA **105**: 6668–6672. doi:10.1073/pnas.0709472105

Diamond, S. E., and L. D. Chick. 2018. The Janus of macrophysiology: Stronger effects of evolutionary history, but weaker effects of climate on upper thermal limits are reversed for lower thermal limits in ants. Curr. Zool. **64**: 223–230. doi:10.1093/cz/zox072

Dowd, W. W., F. A. King, and M. W. Denny. 2015. Thermal variation, thermal extremes and the physiological performance of individuals. J. Exp. Biol. **218**: 1956–1967. doi:10.1242/jeb.114926

Eppley, R. W. 1972. Temperature and phytoplankton growth in the sea. Fish. Bull. **70**: 1063–1085.

Falkowski, P. G., R. T. Barber, and V. Smetacek. 1998. Biogeochemical controls and feedbacks on ocean primary production. Science **281**: 200–206. doi:10.1126/science.281.5374.200

Field, C. B., M. J. Behrenfeld, J. T. Randerson, and P. Falkowski. 1998. Primary production of the biosphere: Integrating terrestrial and oceanic components. Science **281**: 237–240. doi:10.1126/science.281.5374.237

Finkel, Z. V., J. Beardall, K. J. Flynn, A. Quigg, T. A. V. Rees, and J. A. Raven. 2010. Phytoplankton in a changing world: Cell size and elemental stoichiometry. J. Plankton Res. **32**: 119–137. doi:10.1093/plankt/fbp098

Fox, J., and S. Weisberg. 2011. An {R} companion to applied regression, 2nd ed. Sage.

Frigstad, H., T. Andersen, D. O. Hessen, L. J. Naustvoll, T. M. Johnsen, and R. G. J. Bellerby. 2011. Seasonal variation in marine C:N:P stoichiometry: Can the composition of seston explain stable Redfield ratios? Biogeosciences **8**: 2917–2933. doi:10.5194/bg-8-2917-2011

García Molinos, J., and others. 2015. Climate velocity and the future global redistribution of marine biodiversity. Nat. Clim. Chang. **6**: 4–11. doi:10.1038/nclimate2769

Geider, R. J., and J. La Roche. 2002. Redfield revisited: Variability of C:N:P in marine microalgae and its biochemical basis. Eur. J. Phycol. **37**: 1–17. doi:10.1017/S0967026201003456

Godhe, A., M. R. McQuoid, I. Karunasagar, I. Karunasagar, and A.-S. Rehnstam-Holm. 2006. Comparison of three common molecular tools for distinguishing among geographically separated clones of the diatom Skeletonema Marinoi Sarno et Zingone (Bacillariophyceae). J. Phycol. **42**: 280–291. doi:10.1111/j.1529-8817.2006.00197.x

Godhe, A., and T. Rynearson. 2017. The role of intraspecific variation in the ecological and evolutionary success of diatoms in changing environments. Philos. Trans. R. Soc. B **372**. doi:10.1098/rstb.2016.0399

Goldenberger, D., I. Perschil, M. Ritzler, and M. Altwegg. 1995. A simple "universal" DNA extraction procedure using SDS and proteinase K is compatible with direct PCR amplification. Genome Res. **4**: 368–370. doi:10.1101/gr.4.6.368

Goldman, J. C. 1986. On phytoplankton growth rates and particulate C: N: P ratios at low light. Limnol. Oceanogr. **31**: 1358–1363. doi:10.4319/lo.1986.31.6.1358

Goldman, J. C., J. J. McCarthy, and D. G. Peavey. 1979. Growth rate influence on the chemical composition of phytoplankton in oceanic waters. Nature **279**: 210–215. doi:10.1038/279210a0

Gotelli, N. J. 1995. A primer of ecology. Sinauer Associates.

Guillard, R. R. L. 1975. Culture of phytoplankton for feeding marine invertebrates, p. 29–60. *In* W. L. Smith and M. H. Chanley [eds.], Culture of marine invertebrate animals: Proceedings—1st conference on culture of marine invertebrate animals Greenport. Springer US.

Hardin, G. 1960. The competitive exclusion principle. Science **131**: 1292–1297. doi:10.1126/science.131.3409.1292

Huey, R. B., and P. E. Hertz. 1984. Is a Jack-of-all-temperatures a master of none? Evolution (N. Y) **38**: 441. doi:10.2307/2408502

Ivlev, V. S. 1945. Biologicheskaya produktivnost'vodoemov. Usp. Sovrem. Biol. **19**: 98–120.

Kaeriyama, H., E. Katsuki, M. Otsubo, M. Yamada, K. Ichimi, K. Tada, and P. J. Harrison. 2011. Effects of temperature and irradiance on growth of strains belonging to seven Skeletonema species isolated from Dokai Bay, southern Japan. Eur. J. Phycol. **46**: 113–124. doi:10.1080/09670262.2011.565128

Karentz, D., and T. J. Smayda. 1984. Temperature and seasonal occurrence patterns of 30 dominant phytoplankton species in Narragansett Bay over a 22-year period (1959-1980). Mar. Ecol. Prog. Ser. **18**: 277–293.

Kearney, M. 2009. Mechanistic niche modelling: Combining physiological and spatial data to predict specie's ranges. Ecol. Lett. **12**: 334–350. doi:10.1111/j.1461-0248.2008.01277.x

Kingsolver, J. G. 2009. The well-temperated biologist. Am. Nat. **174**: 755–768. doi:10.1086/648310

Kirchman, D. L. 2016. Growth rates of microbes in the oceans. Ann. Rev. Mar. Sci. **8**: 285–309. doi:10.1146/annurev-marine-122414-033938

Kooistra, W. H. C. F., D. Sarno, S. Balzano, H. Gu, R. A. Andersen, and A. Zingone. 2008. Global diversity and biogeography of Skeletonema species (Bacillariophyta). Protist **159**: 177–193. doi:10.1016/j.protis.2007.09.004

Lau, M. K. 2013. DTK: Dunnett-Tukey-Kramer Pairwise Multiple Comparison Test Adjusted for Unequal Variances and Unequal Sample Sizes.

Lawrence, C., and S. Menden-deuer. 2012. Drivers of protistan grazing pressure: Seasonal signals of plankton community composition and environmental conditions. Mar. Ecol. Prog. Ser. **459**: 39–52. doi:10.3354/meps09771

Lenaers, G., L. Maroteaux, B. Michot, and M. Herzog. 1989. Dinoflagellates in evolution. A molecular phylogenetic analysis of large subunit ribosomal RNA. J. Mol. Evol. **29**: 40–51. doi:10.1007/BF02106180

Levins, R. 1968. Evolution in changing environments. Princeton Univ. Press.

Listmann, L., M. LeRoch, L. Schlüter, M. K. Thomas, and T. B. H. Reusch. 2016. Swift thermal reaction norm evolution in a key marine phytoplankton species. Evol. Appl. **9**: 1156–1164. doi:10.1111/eva.12362

Litchman, E., K. F. Edwards, C. A. Klausmeier, and M. K. Thomas. 2012. Phytoplankton niches, traits and eco-evolutionary responses to global environmental change. Mar. Ecol. Prog. Ser. **470**: 235–248. doi:10.3354/meps09912

Martiny, A. C., L. Ma, C. Mouginot, J. W. Chandler, and E. R. Zinser. 2016. Interactions between thermal acclimation, growth rate, and phylogeny influence prochlorococcus elemental stoichiometry. PLoS One **11**: 1–12. doi:10.1371/journal.pone.0168291

Miralto, A., and others. 1999. The insidious effect of diatoms on copepod reproduction. Nature **402**: 173–176. doi:10.1038/46023

Montagnes, D. J. S., and D. J. Franklin. 2001. Effect of temperature on diatom volume, growth rate, and carbon and nitrogen content: Reconsidering some paradigms. Limnol. Oceanogr. **46**: 2008–2018. doi:10.4319/lo.2001.46.8.2008

Moreno, A. R., and A. C. Martiny. 2018. Ecological stoichiometry of ocean plankton. Ann. Rev. Mar. Sci. **10**: 43–69. doi:10.1146/annurev-marine-121916-063126

Nixon, S. W., R. W. Fulweiler, B. A. Buckley, S. L. Granger, B. L. Nowicki, and K. M. Henry. 2009. The impact of changing climate on phenology, productivity, and benthic—pelagic coupling in Narragansett Bay. Estuar. Coast. Shelf Sci. **82**: 1–18. doi:10.1016/j.ecss.2008.12.016

Norberg, J. 2004. Biodiversity and ecosystem functioning: A complex adaptive systems approach. Limnol. Oceanogr. **49**: 1269–1277. doi:10.4319/lo.2004.49.4_part_2.1269

O'Donnell, D. R., C. R. Hamman, E. C. Johnson, C. T. Kremer, C. A. Klausmeier, and E. Litchman. 2018. Rapid thermal adaptation in a marine diatom reveals constraints and trade-offs. Glob. Chang. Biol. **24**: 4554–4565. doi:10.1111/gcb.14360

Padfield, D., G. Yvon-Durocher, A. Buckling, S. Jennings, and G. Yvon-Durocher. 2016. Rapid evolution of metabolic traits explains thermal adaptation in phytoplankton. Ecol. Lett. **19**: 133–142. doi:10.1111/ele.12545

Poloczanska, E. S., and others. 2013. Global imprint of climate change on marine life. Nat. Clim. Chang. **3**: 919–925. doi:10.1038/nclimate1958

R Core Team. 2017. R: A Language and Environment for Statistical Computing.

Rynearson, T. 2019*a*. Thermal growth for Skeletonema species as analyzed in Anderson and Rynearson, 2020. Biol. Chem. Oceanogr. Data Manag. Off. doi:10.1575/1912/bco-dmo.774996.1

Rynearson, T. 2019*b*. Elemental carbon and nitrogen data for Skeletonema species as analyzed in Anderson and Rynearson, 2020. Biol. Chem. Oceanogr. Data Manag. Off. doi:10.1575/1912/bco-dmo.780386.1

Rynearson, T. A., and E. V. Armbrust. 2005. Maintenance of clonal diversity during a spring bloom of the centric diatom *Ditylum brightwellii*. Mol. Ecol. **14**: 1631–1640. doi:10.1111/j.1365-294X.2005.02526.x

Sailley, S. F., L. Polimene, A. Mitra, A. Atkinson, and J. I. Allen. 2015. Impact of zooplankton food selectivity on plankton dynamics and nutrient cycling. J. Plankton Res. **37**: 519–529. doi:10.1093/plankt/fbv020

Sarno, D., L. K. Medlin, I. Percopo, and A. Zingone. 2005. Diversity in the genus Skeletonema (Bacillariophyceae). II. An assessment of the taxonomy of S. costatum-like species with the description of four new species. J. Phycol. **41**: 151–176. doi:10.1111/j.1529-8817.2005.04067.x

Schaum, C. E., A. Buckling, N. Smirnoff, D. J. Studholme, and G. Yvon-Durocher. 2018. Environmental fluctuations accelerate molecular evolution of thermal tolerance in a marine diatom. Nat. Commun. **9**: 1–14. doi:10.1038/s41467-018-03906-5

Scholin, C. a., M. Herzog, M. Sogin, and D. M. Anderson. 1994. Identification of group-specific and strain-specific genetic-markers for globally distributed Alexandrium (Dinophyceae). II. Sequence analysis of a fragment of the LSU rRNA gene. J. Phycol. **30**: 999–1011. doi:10.1111/j.0022-3646.1994.00999.x

Sjöqvist, C., A. Godhe, P. R. Jonsson, L. Sundqvist, and A. Kremp. 2015. Local adaptation and oceanographic connectivity patterns explain genetic differentiation of a marine diatom across the North Sea-Baltic Sea salinity gradient. Mol. Ecol. **24**: 2871–2885. doi:10.1111/mec.13208

Sterner, R. W., and J. J. Elser. 2002. Ecological stoichiometry: The biology of elements from molecules to the biosphere. Princeton Univ. Press.

Sunagawa, S., and others 2015. Structure and function of the global ocean microbiome. Science **348**: 1261359. doi:10.1126/science.1261359

Sunday, J. M., A. E. Bates, and N. K. Dulvy. 2012. Thermal tolerance and the global redistribution of animals. Nat. Clim. Chang. **2**: 686–690. doi:10.1038/nclimate1539

Taylor, R. L., K. Abrahamsson, A. Godhe, and S. Å. Wängberg. 2009. Seasonal variability in polyunsaturated aldehyde production potential among strains of Skeletonema marinoi (Bacillariophyceae). J. Phycol. **45**: 46–53. doi:10.1111/j.1529-8817.2008.00625.x

Thomas, M. K., C. T. Kremer, C. A. Klausmeier, and E. Litchman. 2012. A global pattern of thermal adaptation in marine phytoplankton. Science **338**: 1085–1088. doi:10.1126/science.1224836

Thompson, P. A., M. Guo, and P. J. Harrison. 1992. Effects of variation in temperature. I. on the biochemical composition of eight species of marine phytoplankton. J. Phycol. **28**: 481–488. doi:10.1111/j.0022-3646.1992.00481.x

Vargas, C., and others. 2015. Eukaryotic plankton diversity in the sunlit ocean. Science **348**: 1–12. doi:10.1126/science.1261605

Whittaker, K. A., D. R. Rignanese, R. J. Olson, and T. A. Rynearson. 2012. Molecular subdivision of the marine diatom *Thalassiosira rotula* in relation to geographic distribution, genome size, and physiology. BMC Evol. Biol. **12**: 209. doi:10.1186/1471-2148-12-209

Wickham, H. 2016. ggplot2: Elegant graphics for data analysis. New York: Springer-Verlag.

Windecker, L. A. 2010. Ten years of phytoplankton species abundance patterns in mid-Narragansett Bay, Rhode-Island: 1999–2008. Masters Thesis **53**: 160.

Yvon-Durocher, G., M. Dossena, M. Trimmer, G. Woodward, and A. P. Allen. 2015. Temperature and the biogeography of algal stoichiometry. Glob. Ecol. Biogeogr. **24**: 562–570. doi:10.1111/geb.12280

Zar, J. H. 1996. Biostatistical analysis. Prentice-Hall.

Conflict of interest

None declared.